Models and Technologies

Molecular Cancer Therapeutics

Identification of Circadian Determinants of Cancer Chronotherapy through *In Vitro* Chronopharmacology and Mathematical Modeling

Sandrine Dulong[1,2], Annabelle Ballesta[3,4], Alper Okyar[1,2,5], and Francis Lévi[1,2,3,4,6]

Abstract

Cancer chronotherapy aims at enhancing tolerability and efficacy of anticancer drugs through their delivery according to circadian clocks. However, mouse and patient data show that lifestyle, sex, genetics, drugs, and cancer can modify both host circadian clocks and metabolism pathways dynamics, and thus the optimal timing of drug administration. The mathematical modeling of chronopharmacology could indeed help moderate optimal timing according to patient-specific determinants. Here, we combine *in vitro* and *in silico* methods, in order to characterize the critical molecular pathways that drive the chronopharmacology of irinotecan, a topoisomerase I inhibitor with complex metabolism and known activity against colorectal cancer. Large transcription rhythms moderated drug bioactivation, detoxification, transport, and target in synchronized colorectal cancer cell cultures. These molecular rhythms translated into statistically significant changes in pharmacokinetics and pharmacodynamics according to *in vitro* circadian drug timing. The top-up of the multiple coordinated chronopharmacology pathways resulted in a four-fold difference in irinotecan-induced apoptosis according to drug timing. Irinotecan cytotoxicity was directly linked to clock gene *BMAL1* expression: The least apoptosis resulted from drug exposure near *BMAL1* mRNA nadir ($P < 0.001$), whereas clock silencing through siBMAL1 exposure ablated all the chronopharmacology mechanisms. Mathematical modeling highlighted circadian bioactivation and detoxification as the most critical determinants of irinotecan chronopharmacology. *In vitro–in silico* systems chronopharmacology is a new powerful methodology for identifying the main mechanisms at work in order to optimize circadian drug delivery. *Mol Cancer Ther; 14(9); 2154–64. ©2015 AACR.*

Introduction

Most biologic functions in experimental rodents and humans are rhythmically moderated by the Circadian Timing System (CTS) over 24 hours (1). The CTS is constituted of a network of genetic cellular circadian clocks which are coordinated by the suprachiasmatic nuclei, a hypothalamic pacemaker, through the generation of rhythmic physiology (2). The CTS further controls drug metabolism and transport, as well as cell-cycle progression, DNA repair, and apoptosis in experimental rodents and in humans. As a result, drug pharmacokinetics (PK) and/or pharmacodynamics (PD) can vary as a function of dosing time in whole mammalian organisms, as shown for several hundreds of medications (3).

Circadian timing is especially relevant for anticancer drugs whose optimal dose and delivery schedule are most critical for safely achieving best antitumor efficacy (2). Indeed, up-to-several-fold changes in treatment tolerability and/or efficacy were found according to dosing time for 40 anticancer drugs in rodents (2). Moreover, the administration of anticancer agents at the circadian time when they were the safest also achieved best efficacy both in rodents (4) and in cancer patients (5–8). Large intersubject differences in CTS further need to be taken into account for the personalization of circadian delivery of cancer treatments (9, 10). Thus, a systematic mapping of the critical pathways of anticancer drug chronopharmacology and their molecular clock control is required for optimizing treatment effects through tailoring circadian drug delivery to individual CTS.

Drug chronopharmacology is modulated at the cellular level by molecular clocks which are constituted by interconnected transcription/translation loops involving 15 clock genes, where *PER2*, *REV-ERBα*, and *BMAL1* play major roles (3). These genes display circadian rhythms in their expression and in turn generate oscillations in several membrane transporters and enzymes involved in drug metabolism, cell cycle, DNA repair, or apoptosis (2, 11, 12). Thus, the CTS could rhythmically control nearly half of the liver metabolome (13), including many DNA synthesis (14) and detoxification pathways (11).

Here, we use a novel systems chronopharmacology approach that combines *in vitro* and *in silico* models, in order to characterize

[1]INSERM, UMR-SO776 "Rythmes biologiques et cancers," CNRS Campus, Villejuif, France. [2]Université Paris-Sud, Orsay, France. [3]Warwick Systems Biology Centre, Coventry, United Kingdom. [4]Cancer Chronotherapy Unit, Warwick Medical School, Coventry, United Kingdom. [5]Istanbul University, Faculty of Pharmacy, Department of Pharmacology, Istanbul, Turkey. [6]Assistance Publique-Hôpitaux de Paris, Unité de Chronothérapie, Département d'oncologie médicale, Hôpital Paul Brousse, Villejuif, France.

Note: Supplementary data for this article are available at Molecular Cancer Therapeutics Online (http://mct.aacrjournals.org/).

Corresponding Author: Francis Lévi, The University of Warwick, Medical School Building, Coventry CV4 7AL, United Kingdom. Phone: 44-0-24-76575132; Fax: 44-0-24-76574637; E-mail: f.levi@warwick.ac.uk

doi: 10.1158/1535-7163.MCT-15-0129

the chronopharmacology of the anticancer drug irinotecan in human colon carcinoma cells. The drug is taken as a model of an anticancer drug with a complex metabolism (Fig. 1; ref. 15). It is indicated against colorectal cancer, despite severe and dose-limiting intestinal and hematologic toxicities (16). Irinotecan efficacy and toxicity displayed circadian rhythms in groups of mice and patients (2, 17). Several genes and proteins involved in irinotecan PK and/or PD display circadian rhythms in mouse liver and/or intestine, including the drug target *Top1* (18), the bioactivation enzymes *Ces1* and *Ces2* (19), the detoxification enzyme *Ugt1a1* (19), and the efflux transporters *Abcb1a*, *Abcb1b*, and *Abcc2* (17, 18, 20–22). Studies in 8 mouse categories, based on differences in sex and genetic background, revealed large differences in irinotecan chronopharmacology. Statistical modeling of 27 circadian gene expression data in liver and colon highlighted the robust prediction of optimal irinotecan timing with a mathematical model of the *Rev-erbα* and *Bmal1* transcription regulatory loop (23).

In contrast with chronopharmacology studies in whole organisms, investigations in circadian synchronized cell culture models could enable systematic and quantitative information to be gathered, so as to precisely determine and model molecular chronopharmacology (24). Here, we conduct such an *in vitro–in silico* circadian investigation of irinotecan PK–PD in synchronized colorectal cancer cells for the first time. Our aim is the identification of the most critical clock-controlled determinants of drug cytotoxicity. Such knowledge would help optimizing circadian drug delivery patterns according to the host and tumor clocks (25, 26).

Materials and Methods

Cell culture

The human colon tumor cell line Caco-2 was obtained from the ATCC in 2007. Cells were grown in DMEM:Ham F12 medium [DMEM:F12 (1:1)] supplemented with an antibiotic cocktail (penicillin 1000 U/L, streptomycin 100 μg/mL), 2 mmol/L glutamine (Fischer Scientific) and FCS (Dutscher; 10%). They were maintained in a humidified atmosphere containing 5% CO_2 at 37°C. For experiments, cells were seeded on Petri dishes at 2,500 cells/cm^2. Two days after confluence, cells were transfected with 10 nmol/L of siRNA of *BMAL1* (NM_001030272, mix of S1616 and S1618 siRNA sequence from Ambion) or of siRNA control using Lipofectamine RNAiMAX transfection reagent (Invitrogen) as recommended by supplier. Six hours after transfection, cells were replaced in normal culture medium for 2 days. Next, circadian synchronization of cells was performed by a serum shock that consisted in a 2-hour exposure to serum-rich medium (DMEM:F12 containing 50% FBS). The beginning of the serum shock defined Time 0 (T0). Then cells were replaced in normal culture medium.

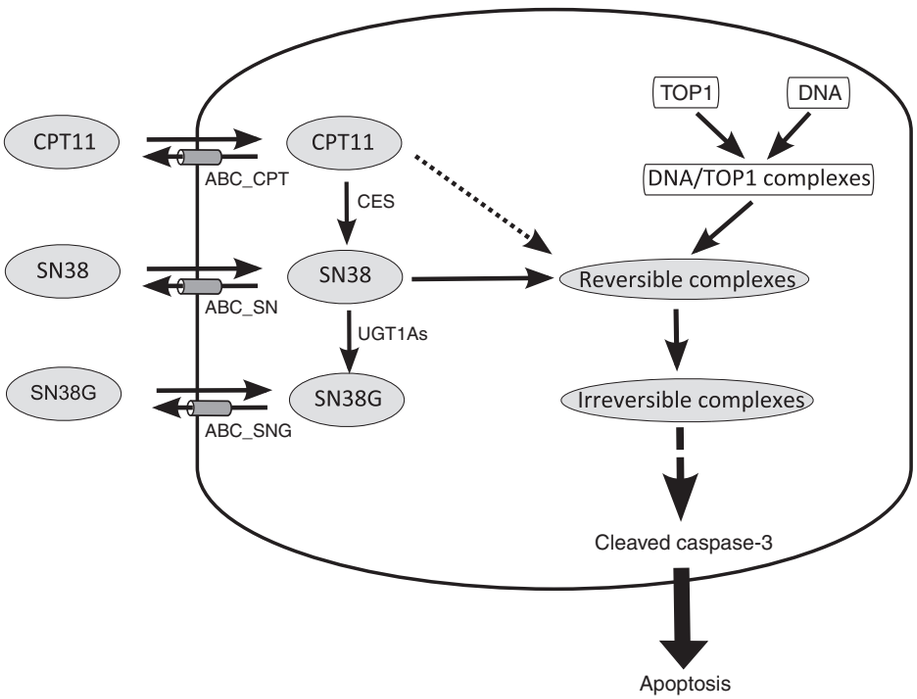

Figure 1.
Scheme depicting molecular PK–PD of irinotecan (CPT11). CPT11 in the extracellular medium diffuses passively through the cell membrane and reaches the intracellular compartment. It is then bioactivated into SN38 through carboxylesterases (CES) enzymatic activities. SN38 is detoxified into SN38G through UGT1As. CPT11, SN38 and SN38G are effluxed outside of the cells by ABC (ATP-binding cassette) transporters (ABC_CPT, ABC_SN, and ABC_SNG, respectively). Topoisomerase 1 (TOP1) is an enzyme that relaxes supercoiled DNA by creating transient DNA/TOP1 complexes. SN38 and CPT11, to a lesser extent, stabilize them into reversible complexes, which may become irreversible after collision with replication or transcription mechanisms. This may trigger the apoptotic machinery though the cleavage of caspase-3, ultimately leading to cell apoptosis. Proteins involved in irinotecan efflux (ABC_CPT, ABC_SN, ABC_SNG), bioactivation (CES), and deactivation (UGT1As), together with irinotecan target (TOP1) present experimentally demonstrated circadian rhythms.

Evaluation and modeling of circadian gene expression

At indicated circadian times (Ts), siRNA-treated synchronized cells were scrapped in guanosine isothiocyanate and frozen at −80°C until RNA extraction. Total RNA was then extracted as described in (27). Reverse transcription was realized with SuperscriptII RT- (Invitrogen). Quantitative PCR was performed with LightCycler 480 using LightCycler 480 SYBR Green I master kit (Roche). Primers used for gene amplification were previously described (24, 28). Hybridization temperature for all the primers was 60°C. Relative quantification of target RNA using *36B4* as reference were realized with Relquant software (Roche).

Circadian gene expressions in synchronized Caco-2 cells were modeled as a damped cosine (24):

$$RNA(t) = M + e^{-\lambda t} A \cos\left(\frac{2\pi}{T}(t-\varphi)\right) \quad (1)$$

The common period T and gene parameters λ, M, A, and φ were simultaneously estimated for all genes, under control or *BMAL1* siRNA conditions, using a previously described bootstrap approach (ref. 24; Supplementary Table S1). We removed the first 2 data points at 0 and 4 hours from the parameter estimation procedure as purely circadian variations may be perturbed by the seric shock during the first 4 hours. Indeed, this allowed us to achieve a better fit to equation (1) compared with taking into account all data points.

Treatments with irinotecan and evaluation by HPLC

Irinotecan was purchased from Pfizer. For chronoPK experiments, Caco-2 cells were first exposed to control or *BMAL1* siRNA before being synchronized. Cells were then exposed to 75 μmol/L of CPT11 for 6 hours starting at T2, 14, and 20. Irinotecan was added to the culture medium 6 hours before incubation with cells in order to reach the lactone–carboxylate equilibrium. CPT11 and SN38 extra- and intracellular concentrations were measured by the method of high-performance liquid chromatography (HPLC) described (24).

Evaluation of TOP1 cleavable complexes

For circadian assessment of TOP1 complexes, siRNA-treated synchronized cells (1×10^6 to 10×10^6) were exposed to SN38 (0.1 μmol/L) at 37°C during 30 minutes at indicated CTS. DNA–topoisomerase I complexes were then measured by a slot-blot method adapted from Subramanian and colleagues (26) using the Topo I Link Kit (TopoGen) as previously described (24).

Viability and apoptosis measurements

Cell viability and apoptosis measurements were performed using respectively the CellTiter-Glo Kit and caspase 3/7-Glo Kit (Promega). Cells were seeded in 96-well plates treated with control and *BMAL1* siRNA and synchronized and treated 3 days after confluence with CPT11 (85 μg/mL) during 2 hours starting at T2, 14, 20, and 28. Twenty-four hours after treatment, reaction buffer was added in each well and bioluminescence was measured using Luminometer (Berthold Technologies). Apoptosis percentages compared with untreated cells were then normalized to cell viability percentages.

Statistical analysis

Statistically significant differences according to circadian time and experimental condition were tested with multiple-way ANOVA, including Scheffe contrast test, using the SPSS software (v.16.0) for Windows software. Circadian rhythmicity of mRNA levels was validated by statistical tests of null amplitude (See Supplementary Information). The Pearson χ^2 test was used to measure the goodness of the fit of the irinotecan PK–PD model.

CPT11 PK–PD model and parameter estimation

Model design. CPT11 molecular PK–PD was represented by a mathematical model on the basis of ordinary differential equations that were solved using the *ode15s* MATLAB function. The final model is an extended version of a previously published one (24). The equations describing the dynamics of CPT11, SN38, and SN38G extra- and intracellular concentrations together with those of DNA/TOP1, reversible and irreversible SN38/DNA/TOP1 complexes were kept unchanged. To account for the fact that irreversible DNA damage may trigger the apoptotic machinery, we supplemented the existing model with the following equation that phenomenologically computes the percentage of apoptotic cells *Apop*:

$$\frac{d\,Apop}{dt} = k_{\text{apop}} I_{\text{compl}} \quad (2)$$

The state variable I_{compl} represents the intracellular concentration of irreversible SN38/DNA/TOP1 complexes and the parameter k_{apop} accounts for DNA repair mechanisms and apoptosis pathways which both display daily variations (29). Therefore, we allow k_{apop} to have circadian rhythms:

$$k_{\text{apop}}(t) = M^{\text{apop}} + A^{\text{apop}} \cos\left(\frac{2\pi}{T}(t-\varphi^{\text{apop}})\right) \quad (3)$$

Circadian variations are also assumed for the enzymatic activity of irinotecan bioactivation (CES), SN38 detoxification (UGT1As), and of the cellular efflux of irinotecan (ABC_CPT) and SN38 (ABC_SN) in agreement with experimental results of Fig. 1 and with literature (23, 24, 30). Protein activities were modeled by a cosine function of common period T as determined in the mRNA studies:

$$\text{Activity}(t) = M^{\text{activity}} + A^{\text{activity}} \cos\left(\frac{2\pi}{T}(t-\varphi^{\text{activity}})\right) \quad (4)$$

Parameters M^{activity}, A^{activity}, and $\varphi^{\text{activity}}$ were computed for each protein activity in the parameter estimation procedure. No circadian variations were considered for TOP1 as suggested by constant nucleic protein amount (Supplementary Fig. S1).

Model parameter estimation. In total, 21 PK parameters and 12 circadian parameters had to be estimated. TOP1 total protein concentration was set to 70 nmol/L as observed in mouse cells (31). Model parameters were estimated to optimally reproduce the chronoPK results (extra- and intracellular CPT11 and SN38 concentrations, Fig. 2), the percentage of DNA-bound Top1 in presence of SN38 (Fig. 3) and CPT11-induced apoptosis (Fig. 4), in the presence of control or BMAL1 siRNA treatment, for

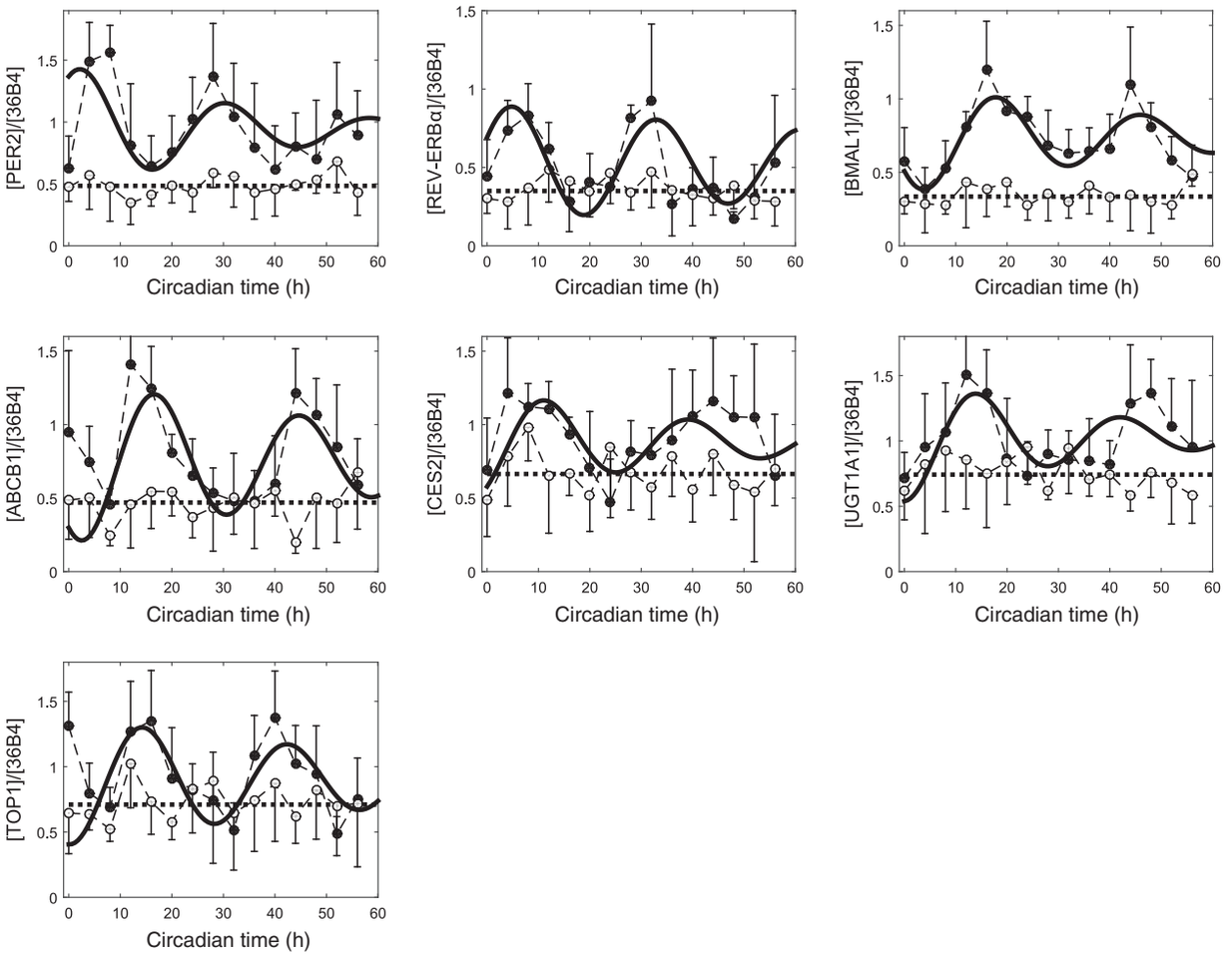

Figure 2.
Circadian rhythms of gene expression in synchronized Caco-2 cells. The mRNA levels of 3 clock genes (*PER2, REV-ERBα, BMAL1*) and 4 genes involved in irinotecan PK–PD (*CES2, ABCB1, UGT1A1, TOP1*) displayed circadian variations in control (black circles) but not in *BMAL1* siRNA-transfected cells (white circles). Experimental results are mean ± SEM of 12 samples from 4 independent experiments. Solid curves represent the best fit of a damped cosine model [equation (1), see Supplementary Table S1, for parameter values).

the 3 studied Ts of exposure (See Supplementary Tables S2 and S3 for final parameter values). Initial search values were set to parameter estimates of the previous version of the model (24). The parameter estimation consisted in a bootstrap approach based on a weighted least-square method, as previously described (24).

Sensitivity analysis. We performed a Sobol variance–based global sensitivity analysis on the model as follows. First, parameters' lower and upper bounds were set to 100-fold lesser and greater than their estimated values and 50,000 parameter sets were generated from cross-sampling by Saltelli's extension of Sobol's method using the MOEA framework (version 2.0, http://www.moeaframework.org/ ref. 32). For each parameter set, the considered model output was computed using MATLAB. Finally, the Sobol analysis function of the MOEA framework was used to compute parameters' total-order sensitivity indices—which represent the contribution to the output variance of the studied parameter including all variances caused by its interactions with other parameters—together with their confidence intervals. Only parameters with a sensitivity of >5% are shown.

We studied the sensitivity of all model parameters—except K_m's of enzymatic reactions—together with that of irinotecan initial concentration and exposure duration (T_{expo}). Irinotecan cytotoxicity was assessed through DNA damage—defined as the sum of reversible and irreversible SN38/DNA/TOP1 complexes formed during irinotecan exposure. Drug-induced apoptosis was not used as an endpoint in sensitivity analysis because it was not mechanistically modeled.

Results

Circadian rhythms of clock genes and control of irinotecan metabolic pathways

The circadian mRNA expression patterns of 3 core clock genes (*PER2*, *REV-ERBα*, *BMAL1*) and 4 critical activation, transport, detoxification, and target genes for irinotecan

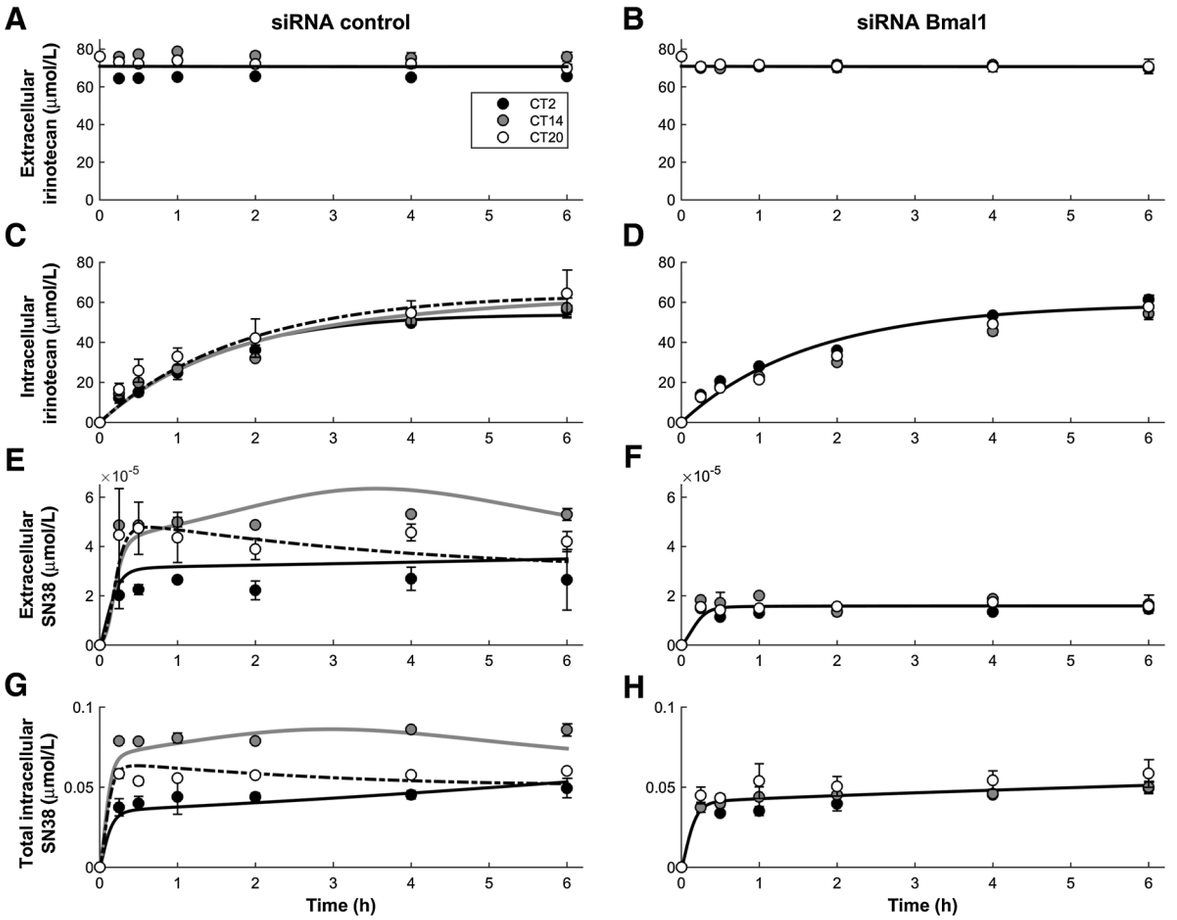

Figure 3.
ChronoPK of irinotecan (CPT11) in control or *BMAL1* siRNA–treated synchronized Caco-2 cells. Dots are experimental results (mean ± SD of data from 3 samples). Solid lines correspond to the PK–PD model best fit for CT2 (black), CT14 (gray), and CT20 (dashed). Total intracellular SN38 stands for the sum of free and DNA-bound metabolite concentration. In A, B, D, F, and H, model simulations for T2, T14, and T20 were superimposed.

metabolism (*CES2*, *ABCB1*, *UGT1A1*, *TOP1*) were first determined in synchronized human colon cancer Caco-2 cells in the presence of control or *BMAL1* siRNA. In cells treated with control siRNA, the 3 clock genes and the 4 pharmacologic genes displayed circadian rhythms in their mRNA expression with amplitude values *A* ranging from 40% to 80% of mean values *M* (Figs. 2 and Supplementary Table S1). The common period was estimated to $\tau = 28$ h 06 min (SD, 1 h 41 min). Differences between phases of *BMAL1* and *PER2* and between *BMAL1* and *REV-ERBα* were respectively equal to 13 h 33 min (=0.94 π rad) and 15 h 41 min (=1.1 π rad). Thus, the circadian expression pattern of *BMAL1* was in antiphase to that of *REV-ERBα* and *PER2* in this colon cancer cell line. This finding was consistent with the reciprocal regulation of these 3 clock genes within the molecular circadian clock in healthy cells or tissues (12). We further noticed a mild dampening of the mRNA oscillations in the range of $\lambda \approx 10^{-2}$ per hour, which may account for a slight desynchronization of cells over time. Times of maximal mRNA expressions (acrophases) were located at 11 h 28 min for *CES2*, at 14 h 26 min for *UGT1A1*, at 16 h 51 min for *ABCB1*, and at 14 h 30 min for *TOP1* modulo the period of 28 h 06 (Supplementary Table S1).

As expected, the exposure of Caco-2 cells to *BMAL1* siRNA resulted in a 56% decrease in *BMAL1* mean mRNA expression as compared with controls (Fig. 2). si-BMAL1 exposure completely turned off the circadian oscillations of the mRNA expression of the 3 clock genes and those of the 4 metabolism genes in Caco-2 cell populations (Supplementary Table S1). *BMAL1* silencing also resulted in a 27% to 48% decrease in the mean mRNA level of the other 6 genes of interest—as compared with their respective controls—and reduced mRNA expressions by 48% to 72% at the time of their respective peak expressions (Supplementary Table S1).

Irinotecan chronoPK

The above mRNA circadian expression data in clock-proficient Caco-2 cells were in line with those obtained earlier (24). They led to model and predict that irinotecan toxicity would be least following exposure onset at T2 and highest after treatment initiation at T14 or T20 (24). These 3 circadian timings were used here for testing the relevance of the molecular clock for irinotecan metabolism and cellular PK following irinotecan exposure (75 μg/mL) over 6 hours. The extracellular concentration pattern of irinotecan displayed minor yet statistically significant

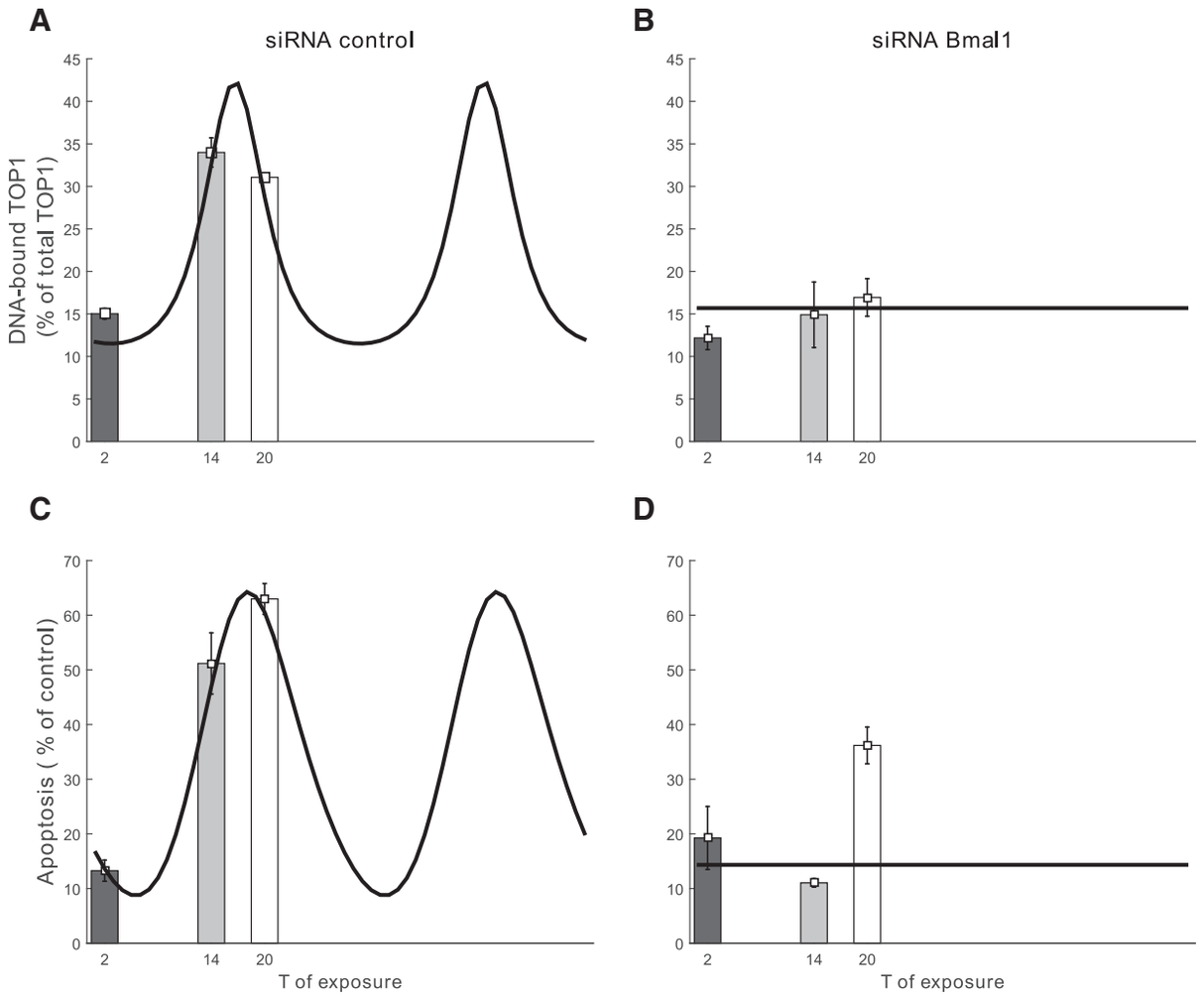

Figure 4.
Circadian variations of SN38-induced TOP1 complexes (A and B) and CPT11-induced apoptosis (C and D) in synchronized Caco-2 cells with a functional clock (left column) or with silenced *BMAL1* (right column). Bars represent experimental data from 3 experiments (mean ± SD). Solid lines depict the model best fit.

differences according to treatment timing in the clock-proficient Caco-2 cells (Fig. 3). Thus, the mean area under the curve over 6 h ($AUC_{0-6\ h}$) of extracellular irinotecan concentration varied according to treatment time (ANOVA, $P = 0.001$). Mean $AUC_{0-6\ h}$ (±SEM) was lowest following treatment at T2 (392.3 ± 2.3 μmol/L·h), intermediate after treatment at T20 (433.0 ± 5.6 μmol/L ·h), and highest after drug exposure at T14 (458.1 ± 5.6 μmol/L·h). However, irinotecan timing did not moderate intracellular irinotecan concentration dynamics or $AUC_{0-6\ h}$ (Fig. 3C and D; ANOVA, $P = 0.117$). In contrast, irinotecan timing profoundly modified both intracellular and extracellular concentration dynamics of SN38, the bioactive metabolite of irinotecan. These differences translated into large and statistically significant changes in both intra- and extracellular $AUC_{0-6\ h}$ of SN38 according to the T of drug exposure ($P < 0.0001$). Mean $AUC_{0-6\ h}$ values of intracellular SN38 (± SEM) ranged from 265.13 ± 4.5 nmol/L·h for cells exposed at T2, to 489.7 ± 2.59 nmol/L·h for those exposed at T20, and 341 ± 3.3 nmol/L·h following treatment at T14. Corresponding values for extracellular SN38 $AUC_{0-6\ h}$ were 0.15 ± 0.004, 0.3 ± 0.003, and 0.26 ± 0.001 nmol/L ·h, respectively. These findings highlighted the key role of the molecular clock for irinotecan and SN38 transport and metabolism.

In sharp contrast, the disruption of the circadian clock with *BMAL1* siRNA completely erased the large dosing time dependencies found in clock-proficient cells (Fig. 3). Indeed, no dosing time dependency was apparent for the extracellular and intracellular concentrations of irinotecan and SN38, as well as for their respective $AUC_{0-6\ h}$ (ANOVA; $P = 0.05$).

Irinotecan dosing at T2 resulted in similar values for intracellular or extracellular SN38 $AUC_{0-6\ h}$ irrespective of clock silencing, with corresponding means close to 250 and 0.07 nmol/L·h, respectively. However, clock silencing markedly decreased irinotecan bioactivation into SN38 after drug exposure at T14 or T20 down to its level found at T2 in clock-proficient cells (Fig. 3E–H).

Circadian variations of TOP1 cleavable complex

We then questioned the relevance of the molecular circadian clock for SN38 molecular PK. The amount of DNA-bound TOP1

protein varied according to SN38 timing with statistical significance in clock-proficient Caco-2 cells (ANOVA, $P < 0.0001$; Fig. 4A). Indeed, mean DNA-bound TOP1 amount nearly doubled between treatment at T2 and T14 ($P = 0.011$) or T20 ($P = 0.02$), whereas differences between T14 and T20 were minor and not statistically significant (ANOVA, $P = 0.86$). In contrast, DNA-bound TOP1 protein amount did not differ according to SN38 timing in clock-defective cells, with amounts similar to those found in clock-proficient cells treated at T2.

Circadian variations of irinotecan-induced apoptosis

The implications of the circadian clock control of molecular chronoPK and chronoPD for drug toxicity was further determined, through the quantification of caspase-3 activation as a marker of drug-induced apoptosis. Clock-proficient cells exposed to control siRNA displayed statistically significant time-dependent apoptosis (ANOVA, $P < 0.0001$; Fig. 4B). Apoptosis induction was increased by 14%, 52%, and 63% following irinotecan treatment at T2, T14, and T20, respectively, as compared with untreated controls. We thus observed a 4.5-fold difference in irinotecan-induced apoptosis as a function of whether irinotecan treatment was initiated at T2 or T20.

Modest time-dependent changes were found according to irinotecan timing in clock-defective cells. No statistically significant difference characterized treatment initiated at T2 or T14 ($P = 0.38$), yet apoptosis induction was largest at T20 as compared with T14 ($P = 0.002$) or T2 ($P = 0.025$). Clock silencing with *BMAL1* siRNA dramatically decreased irinotecan-induced apoptosis by 72% in cells treated at T14 and by 65% in cells treated at T20. In contrast, apoptosis increased by 25% in the siBMAL1 Caco-2 cells treated at T2 as compared with control conditions.

Model-based analysis of irinotecan chronoPK–PD

A comprehensive mathematical analysis of all the above experimental results was implemented. We first fitted the mathematical model of irinotecan molecular chronoPK–PD to the current multidimensional datasets (see Materials and Methods and Supplementary Data). In the presence of *BMAL1* siRNA treatment, all circadian rhythms were assumed to be disrupted—that is all circadian amplitudes were set to zero—and mean protein activities were allowed to be different from control conditions as suggested by differences in the mean mRNA levels of metabolism genes.

The calibrated mathematical model displayed good qualitative and quantitative agreement with all datasets, thus theoretically confirming the circadian disruption through *BMAL1* siRNA (Figs. 3 and 4). The Pearson χ^2 test validated, with a probability $P > 0.975$, that the irinotecan PK–PD model was correctly representing the 3 datasets of irinotecan PK, TOP1 activity, and drug-induced apoptosis measured at T2, T14, and T20 in both control and siBMAL1-exposed cells. The model predicted circadian activities for the proteins involved in irinotecan bioactivation (CES), SN38 detoxification (UGT1As), as well as for those responsible for irinotecan and SN38 efflux (ABC_CPT, ABC_SN) in control conditions. Predicted amplitude values (A^{activity}) ranged from 12.7% to 80% of the corresponding mean values (M^{activity}) and predicted acrophases ($\varphi^{\text{activity}}$) were shifted by 2 h 08 to 20 h 30 as compared with those of the corresponding mRNA expression rhythms (Fig. 5A and Supplementary Table S2). Furthermore, the fitting procedure predicted a circadian rhythm in k_{apop}, the parameter that links drug-induced DNA damage to apoptosis in the model. This finding suggested an important impact of the circadian control of DNA repair and apoptosis genes and proteins for irinotecan cytotoxicity. The best-fit model predicted highest cytotoxicity following drug exposure onset at 17 h 48 min and least if drug exposure timing started at 5 h 24 min modulo the period of 28 h 06 min (Fig. 4C).

In cells exposed to *BMAL1* siRNA, mean activities of irinotecan efflux transporters and UGT1As enzymes were unchanged compared with clock-proficient cells. In contrast, SN38 efflux transporters and irinotecan bioactivation activities were decreased by 17% and 37%, respectively. The k_{apop} model parameter value was increased by 2.85-fold compared with control, a result supporting a greater susceptibility of clock-deficient cells to irinotecan-induced DNA damage (Supplementary Table S2). The comprehensive mathematical model was consistent with all experimental data except the time-dependent changes in irinotecan extracellular concentrations in the clock-proficient cells, which were not well reproduced by the best-fit simulations. An additional *in vitro* chronoPK experiment was thus performed (See Supplementary Fig. S2). Overall, interstudy variability was considered as accounting for the minor discrepancy in irinotecan extracellular dynamics between both experiments.

The influence of model parameters on irinotecan toxicity pattern was assessed through global sensitivity analyses using DNA damage as the main toxicity endpoint (see Materials and Methods). Parameter sensitivity analyses were performed for (i) the circadian timing of irinotecan exposure onset associated to minimal DNA damage and (ii) the circadian amplitude of irinotecan-induced DNA damage, defined as the difference between the mean and the minimum values of the rhythm.

The circadian timing corresponding to least toxicity was mostly determined by the mean value and the circadian amplitude of both SN38 detoxification (UGT1A) and irinotecan bioactivation (CES), whose respective circadian acrophases ranked as first and second most sensitive parameters (Figs. 5B and 6). Irinotecan exposure duration ranked third, and the detoxification and bioactivation circadian amplitudes ranked fourth and fifth, respectively.

The amplitude of the toxicity rhythm was largely determined by the 3 circadian parameters of bioactivation, whose amplitude, mean value, and acrophase ranked as first, second, and fifth most sensitive parameters, respectively (Figs. 5C and 6). DNA complex formation and dissociation parameters also contributed to drug toxicity amplitude as k_{f1} (DNA/TOP1 complex formation), k_{f2} (SN38/DNA/TOP1 complex formation), k_{d1} (DNA/TOP1 complex dissociation), k_{DSB} (irreversible complex formation), and k_{d2} (SN38/DNA/TOP1 complex dissociation), respectively, ranked as third, sixth, seventh, eighth, and ninth parameters.

Discussion

Improving our understanding of the circadian rhythms that govern anticancer drug toxicities and efficacy requires identifying the critical molecular determinants of the circadian control of drug metabolism. To this end, we here investigated the *in vitro* chronopharmacology of irinotecan as a first proof of concept of chronopharmacology in synchronized cancer cell populations. This novel *in vitro–in silico* approach to

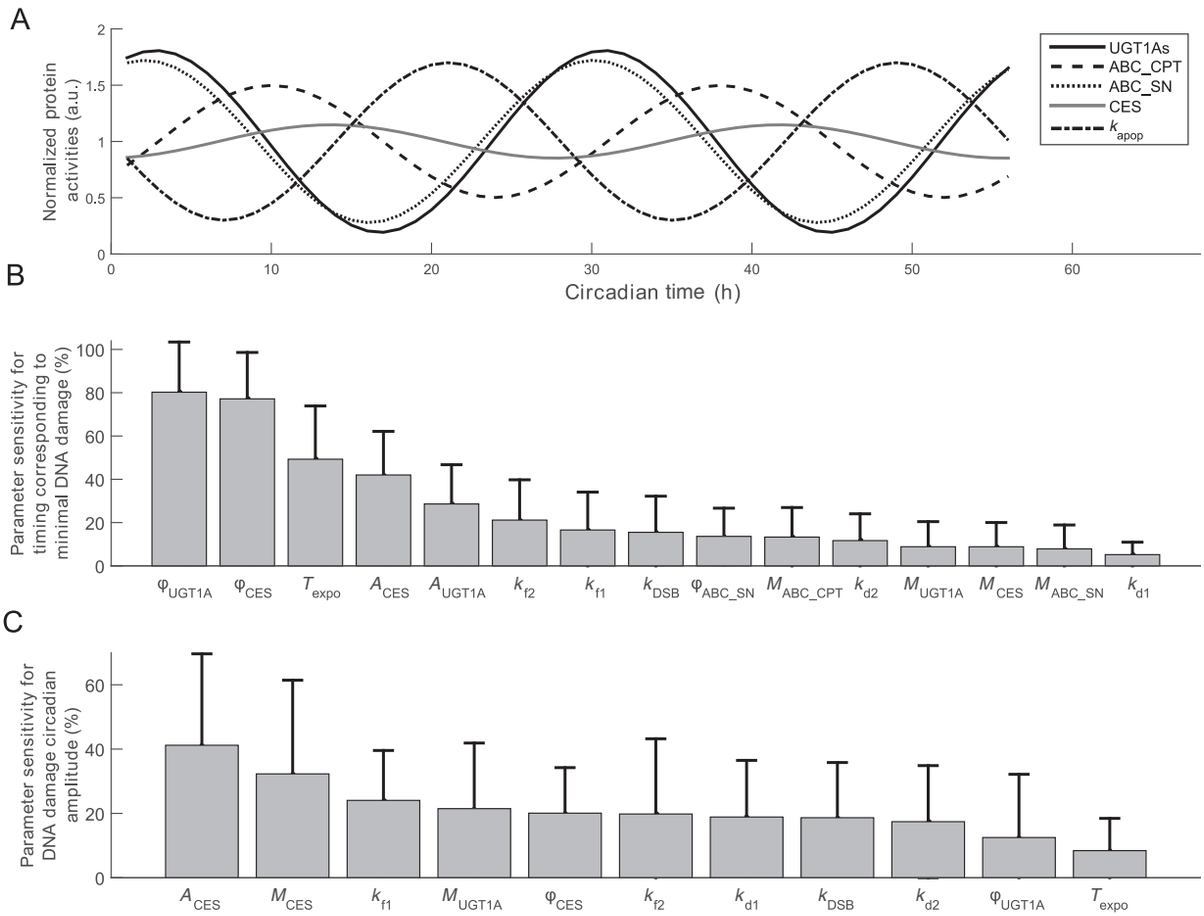

Figure 5.
Model-based predictions of molecular determinants of irinotecan cytotoxicity circadian pattern. A, protein activity circadian rhythms in control cells regarding irinotecan bioactivation (CES), irinotecan efflux (ABC_CPT), SN38 efflux (ABC_SN), SN38 detoxification (UGT1As), and the DNA damage phenotype (k_{apop}). B, parameter sensitivity for irinotecan circadian timing resulting in minimal DNA damage. The circadian phase (φ) of SN38 detoxification (UGT1As) and irinotecan bioactivation (CES) ranked as first and second most sensitive parameters. Their total-order sensitivity indices—that is, the contribution of the corresponding parameter to the change obtained in the minimal toxicity timing when all parameters are varied over their entire range—were equal to 80.2% and 77.2%, respectively. Their circadian amplitudes (A) ranked as fourth and fifth parameters, with indices of 28.6% and 42%, respectively. Irinotecan exposure duration (T_{expo}) also largely influenced the circadian timing corresponding to least cytotoxicity, as its total-order sensitivity indices ranked third and reached 49.3%. C, parameter sensitivity for the amplitude of DNA damage rhythm. This output was largely influenced by the bioactivation genes whose rhythm amplitude (A), mean value (M), and acrophase (φ) ranked as first, second, and fifth most sensitive parameters, with respective indices equal to 41.2%, 32.3%, and 20.1%. Parameters involved in DNA complex formation and dissociation also played role, as k_{f1} (DNA/TOP1 complex formation), k_{f2} (SN38/DNA/TOP1 complex formation), k_{d1} (DNA/TOP1 complex dissociation), k_{DSB} (irreversible complex formation), and k_{d2} (SN38/DNA/TOP1 complex dissociation), respectively, ranked as third, sixth, seventh, eighth, and ninth parameters.

developmental chronotherapeutics should be viewed as aiming to help dissect the relative contribution of the cellular molecular clock and that of systemic factors for the chronopharmacology of irinotecan. Here, circadian rhythms in irinotecan pharmacology and toxicity were found for each studied parameter in synchronized Caco-2 cell cultures and were all ablated following exposure to *BMAL1* siRNA. Thus, irinotecan chronopharmacology resulted from the control of its metabolism by the molecular circadian clock. Moreover, irinotecan cytotoxicity appeared to be positively correlated to the expression level of clock gene *BMAL1*, both in clock-proficient and in clock-deficient cells. In contrast, the cytotoxicity of oxaliplatin, another effective anticancer drug against colorectal cancer, reportedly displayed a negative correlation with *BMAL1* expression level (33). Taken together, the findings suggest that *BMAL1* tumor expression could help select the most effective drug for a given patient.

The physiologically based model of irinotecan chronoPK–PD closely agreed with experimental results. Model parameter sensitivity analyses highlighted the overall predominant influence of bioactivating CES and detoxifying UGT1As circadian rhythms on irinotecan chronotoxicity pattern. The mRNA expression circadian rhythms were in good agreement with previously published data (24). The circadian acrophases of *BMAL1*, *TOP1*, *UGT1A1*, and *ABCB1* were indeed similar to those earlier found in a separate study, whereas those of *PER2*, *REV-ERBα* and *CES2* differed by less than $\frac{\pi}{2}$ rad (Supplementary Fig. S3). The mathematical model of irinotecan chronoPK–PD, which was initially designed

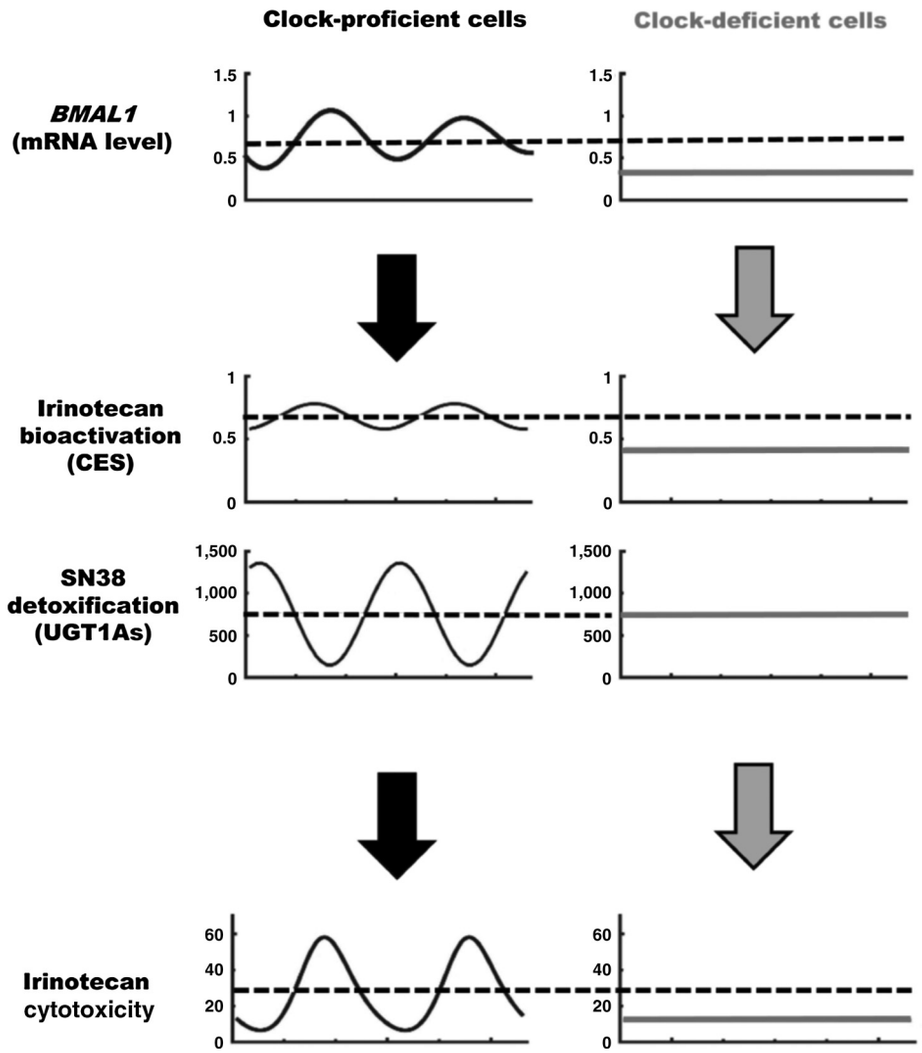

Figure 6.
Scheme summarizing the main molecular determinants of irinotecan cytotoxicity according to clock proficiency (left column) or clock deficiency (right column). Clock-proficient cells display a rhythmic *BMAL1* mRNA expression (first row), which regulates irinotecan bioactivation through CES activities (second row) and SN38 detoxification through UGT1A activities (third row), resulting in circadian pattern in irinotecan cytotoxicity (fourth row). Clock-deficient cells display flat patterns for all the parameters. The mean value of irinotecan bioactivation is reduced as compared with clock-proficient cells, which results in low cytotoxicity. Note the tight temporal coordination of bioactivation and detoxification in clock-proficient cells. The positive relation between *BMAL1* mRNA expression and irinotecan cytotoxicity both in clock-proficient and in clock-deficient cells supports the potential relevance of *BMAL1* as a predictive biomarker of irinotecan cytotoxicity.

for unsynchronized Caco-2 cells, successfully fitted the current datasets in synchronized cells, a step that further validated the model structure. New parameter estimates were obtained here, which highlighted kinetics differences between synchronized and unsynchronized cells, thus providing an opportunity for differentiating chronopharmacology in healthy and malignant tissues (Supplementary Table S3).

An interesting added value of the model involved its ability to accurately predict the circadian patterns in the main metabolism proteins, based upon gene and pharmacology data. The estimated protein acrophases were shifted by 1 h 24 min to 20 h 30 min relative to those found for the corresponding genes. Intervals ranging from 0 to 20 hours (modulo, 24 hours) were previously reported between several mRNA and protein expressions in mouse tissues (30). The model predictions based on synchronized Caco-2 data were rather consistent with mouse liver data, following the normalization of the circadian period to 24 hours for the Caco-2 cells. Thus, the model predicted a time lag of 14 hours for UGT1As mRNA and protein expression rhythms, whereas it was equal to 15 hours for *Ugt1a1* in mouse liver (30). Similarly, the model predicted a 22-hour time lag between CES mRNA and protein, which differed from mouse liver *Ces2* by only 4 hours (30).

The slight shift between the circadian rhythm in irinotecan-induced DNA-bound TOP1 and that in extent of apoptosis suggested the occurrence of an additional circadian control of DNA repair and apoptosis processes. The best-fit mathematical model indeed included a non-zero circadian amplitude for the parameter k_{apop}, which represents the DNA damage response phenotype, including the *P53* network, DNA repair and, eventually, apoptosis. Besides its regulatory effect on apoptosis, *P53* also regulates the molecular clock so that *P53* mutation could modify the circadian rhythms of the protein activities involved in irinotecan chronopharmacology and therefore alter the circadian pattern in irinotecan cytotoxicity (29, 34).

Altogether, the current model-driven chronopharmacology study has established the molecular bases of irinotecan chronopharmacology, through setting up a comprehensive

mechanistic circadian PK–PD model for this drug. Several levels of prediction have been confirmed, regarding the circadian control of gene transcription and proteins, based on a recent literature survey. Moreover, the temporal relation between low *BMAL1* expression and low irinotecan toxicity found *in vitro* was in good agreement with experimental studies in mice regarding the circadian toxicity pattern of this drug as well (23). The results advocate thus for the model validity and accuracy, which now deserves further prospective adjustments in selected experimental models, before clinical testing of personalized chronopharmacology delivery in cancer patients.

Disclosure of Potential Conflicts of Interest

No potential conflicts of interest were disclosed.

Authors' Contributions

Conception and design: S. Dulong, A. Ballesta, A. Okyar, F. Lévi
Development of methodology: S. Dulong, A. Ballesta, F. Lévi
Acquisition of data (provided animals, acquired and managed patients, provided facilities, etc.): S. Dulong, F. Lévi
Analysis and interpretation of data (e.g., statistical analysis, biostatistics, computational analysis): S. Dulong, A. Ballesta, A. Okyar, F. Lévi
Writing, review, and/or revision of the manuscript: S. Dulong, A. Ballesta, A. Okyar, F. Lévi
Administrative, technical, or material support (i.e., reporting or organizing data, constructing databases): S. Dulong, A. Ballesta
Study supervision: S. Dulong, A. Ballesta, F. Lévi

Acknowledgments

The authors thank Dr. Jean Clairambault for his role in the initiation of this project and subsequent fruitful discussions.

Grant Support

This work was co-funded by the ARC (CR109/8003) to F. Lévi, the European Commission through the specific targeted research project TEMPO (*LSHG-CT-2006-037543*) to all authors, *ERASysBio+ (C5Sys, LHSB-2010-005137)* to F. Lévi and S. Dulong, CaSyM (HEALTH-F4-2012-305033) to A. Ballesta and F. Lévi, and the research fund of Istanbul University (N-7762/2010) to A. Okyar.

The costs of publication of this article were defrayed in part by the payment of page charges. This article must therefore be hereby marked *advertisement* in accordance with 18 U.S.C. Section 1734 solely to indicate this fact.

Received February 11, 2015; revised May 18, 2015; accepted June 23, 2015; published OnlineFirst July 3, 2015.

References

1. Dibner C, Schibler U, Albrecht U. The mammalian circadian timing system: organization and coordination of central and peripheral clocks. Annu Rev Physiol 2010;72:517–49.
2. Levi F, Okyar A, Dulong S, Innominato PF, Clairambault J. Circadian timing in cancer treatments. Annu Rev Pharmacol Toxicol 2010;50: 377–421.
3. Levi F, Schibler U. Circadian rhythms: mechanisms and therapeutic implications. Annu Rev Pharmacol Toxicol 2007;47:593–628.
4. Ortiz-Tudela E, Mteyrek A, Ballesta A, Innominato PF, Levi F. Cancer chronotherapeutics: experimental, theoretical, and clinical aspects. Handb Exp Pharmacol 2013:261–88.
5. Innominato PF, Giacchetti S, Bjarnason GA, Focan C, Garufi C, Coudert B, et al. Prediction of overall survival through circadian rest-activity monitoring during chemotherapy for metastatic colorectal cancer. Int J Cancer 2012;131:2684–92.
6. Innominato PF, Giacchetti S, Moreau T, Bjarnason GA, Smaaland R, Focan C, et al. Fatigue and weight loss predict survival on circadian chemotherapy for metastatic colorectal cancer. Cancer 2013;119:2564–73.
7. Innominato PF, Roche VP, Palesh OG, Ulusakarya A, Spiegel D, Levi FA. The circadian timing system in clinical oncology. Ann Med 2014; 46:191–207.
8. Mormont MC, Levi F. Circadian-system alterations during cancer processes: a review. Int J Cancer 1997;70:241–7.
9. Ortiz-Tudela E, Iurisci I, Beau J, Karaboue A, Moreau T, Rol MA, et al. The circadian rest-activity rhythm, a potential safety pharmacology endpoint of cancer chemotherapy. Int J Cancer 2014;134:2717–25.
10. Roche VP, Mohamad-Djafari A, Innominato PF, Karaboue A, Gorbach A, Levi FA. Thoracic surface temperature rhythms as circadian biomarkers for cancer chronotherapy. Chronobiol Int 2014;31: 409–20.
11. Gachon F, Olela FF, Schaad O, Descombes P, Schibler U. The circadian PAR-domain basic leucine zipper transcription factors DBP, TEF, and HLF modulate basal and inducible xenobiotic detoxification. Cell Metab 2006;4:25–36.
12. Panda S, Antoch MP, Miller BH, Su AI, Schook AB, Straume M, et al. Coordinated transcription of key pathways in the mouse by the circadian clock. Cell 2002;109:307–20.
13. Eckel-Mahan KL, Patel VR, Mohney RP, Vignola KS, Baldi P, Sassone-Corsi P. Coordination of the transcriptome and metabolome by the circadian clock. Proc Natl Acad Sci U S A 2012;109:5541–6.
14. Fustin JM, Doi M, Yamada H, Komatsu R, Shimba S, Okamura H. Rhythmic nucleotide synthesis in the liver: temporal segregation of metabolites. Cell Rep 2012;1:341–9.
15. Pommier Y. Topoisomerase I inhibitors: camptothecins and beyond. Nat Rev Cancer 2006;6:789–802.
16. Gilbert DC, Chalmers AJ, El-Khamisy SF. Topoisomerase I inhibition in colorectal cancer: biomarkers and therapeutic targets. Br J Cancer 2012; 106:18–24.
17. Ahowesso C. Approche expérimentale de la personnalisation de la chronothérapeutique par irinotecan. Université Paris 2011.
18. Kuramoto Y, Hata K, Koyanagi S, Ohdo S, Shimeno H, Soeda S. Circadian regulation of mouse topoisomerase I gene expression by glucocorticoid hormones. Biochem Pharmacol 2006;71: 1155–61.
19. Ahowesso C, Li XM, Zampera S, Peteri-Brunback B, Dulong S, Beau J, et al. Sex and dosing-time dependencies in irinotecan-induced circadian disruption. Chronobiol Int 2011;28:458–70.
20. Ando H, Yanagihara H, Sugimoto K, Hayashi Y, Tsuruoka S, Takamura T, et al. Daily rhythms of P-glycoprotein expression in mice. Chronobiol Int 2005;22:655–65.
21. Okyar A, Piccolo E, Ahowesso C, Filipski E, Hossard V, Guettier C, et al. Strain- and sex-dependent circadian changes in abcc2 transporter expression: implications for irinotecan chronotolerance in mouse ileum. PLoS One 2011;6:e20393.
22. Filipski E, Berland E, Ozturk N, Guettier C, van der Horst GT, Levi F, et al. Optimization of irinotecan chronotherapy with P-glycoprotein inhibition. Toxicol Appl Pharmacol 2014;274: 471–9.
23. Li XM, Mohammad-Djafari A, Dumitru M, Dulong S, Filipski E, Siffroi-Fernandez S, et al. A circadian clock transcription model for the personalization of cancer chronotherapy. Cancer Res 2013;73: 7176–88.
24. Ballesta A, Dulong S, Abbara C, Cohen B, Okyar A, Clairambault J, et al. A combined experimental and mathematical approach for molecular-based optimization of irinotecan circadian delivery. PLoS Comput Biol 2011;7: e1002143.
25. Goldwasser F, Bae I, Valenti M, Torres K, Pommier Y. Topoisomerase I-related parameters and camptothecin activity in the colon carcinoma cell lines from the National Cancer Institute anticancer screen. Cancer Res 1995;55:2116–21.

26. Subramanian D, Kraut E, Staubus A, Young DC, Muller MT. Analysis of topoisomerase I/DNA complexes in patients administered topotecan. Cancer Res 1995;55:2097–103.
27. Chomczynski P, Sacchi N. Single-step method of RNA isolation by acid guanidinium thiocyanate-phenol-chloroform extraction. Anal Biochem 1987;162:156–9.
28. Teboul M, Delaunay F. [No hierarchy in mammalian circadian system]. Med Sci (Paris) 2004;20:628–9.
29. Sancar A, Lindsey-Boltz LA, Kang TH, Reardon JT, Lee JH, Ozturk N. Circadian clock control of the cellular response to DNA damage. FEBS Lett 2010;584:2618–25.
30. Mauvoisin D, Wang J, Jouffe C, Martin E, Atger F, Waridel P, et al. Circadian clock-dependent and -independent rhythmic proteomes implement distinct diurnal functions in mouse liver. Proc Natl Acad Sci U S A 2014;111:167–72.
31. Schwanhausser B, Busse D, Li N, Dittmar G, Schuchhardt J, Wolf J, et al. Global quantification of mammalian gene expression control. Nature 2011;473:337–42.
32. Saltelli A, Ratto M, Andres T, Campolongo F, Cariboni J, Gatelli D, et al. Global sensitivity analysis. The primer. Chichester, England: Wiley; 2008.
33. Zeng ZL, Luo HY, Yang J, Wu WJ, Chen DL, Huang P, et al. Overexpression of the circadian clock gene Bmal1 increases sensitivity to oxaliplatin in colorectal cancer. Clin Cancer Res 2014;20:1042–52.
34. Miki T, Matsumoto T, Zhao Z, Lee CC. p53 regulates Period2 expression and the circadian clock. Nat Commun 2013;4:2444.